

# SimpleTool: Parallel Decoding for Real-Time LLM Function Calling

Xiaoxin Shi<sup>1,2</sup> Jiaxin Wan<sup>2</sup> Linkang Dong<sup>2</sup> Wei Jiang<sup>2</sup> Yue Liu<sup>2</sup> Zengfeng Huang<sup>2,3</sup>

 [GitHub: https://github.com/HaxxorCialtion/SimpleTool](https://github.com/HaxxorCialtion/SimpleTool)

 [Hugging Face: https://huggingface.co/Cialtion/SimpleTool](https://huggingface.co/Cialtion/SimpleTool)

 [ModelScope: https://www.modelscope.cn/models/cialtion/SimpleTool](https://www.modelscope.cn/models/cialtion/SimpleTool)

[cialtion737410@sjtu.edu.cn](mailto:cialtion737410@sjtu.edu.cn) [huangzf@fudan.edu.cn](mailto:huangzf@fudan.edu.cn)

<sup>1</sup>Shanghai Jiao Tong University, Shanghai, China

<sup>2</sup>Shanghai Innovation Institute, Shanghai, China

<sup>3</sup>Fudan University, Shanghai, China

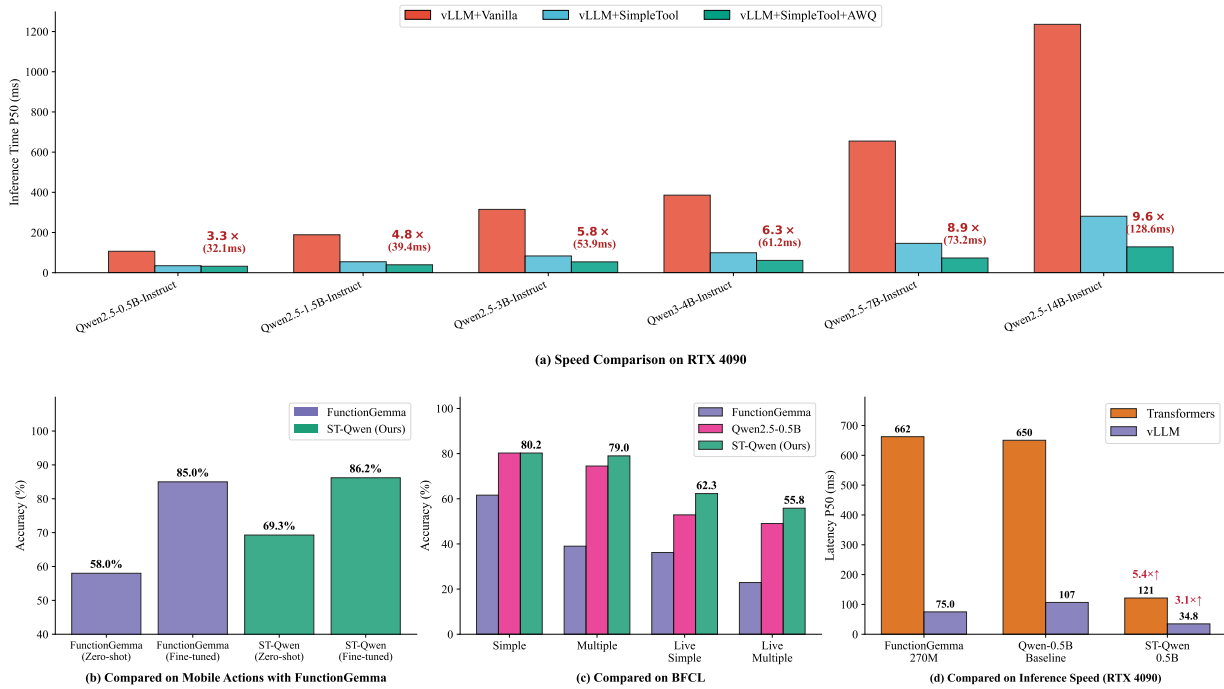


**Figure 1.** Performance Overview of SimpleTool. **(a)** End-to-end inference latency comparison across various Qwen model sizes on an RTX 4090. Our method achieves up to a **9.6×** speedup. **(b)** Accuracy comparison against FunctionGemma on the Mobile Actions benchmark. **(c)** Accuracy comparison on the BFCL benchmark among FunctionGemma, the Qwen2.5-0.5B baseline, and our ST-Qwen-0.5B. **(d)** Inference latency comparison across different models and frameworks (Transformers vs. vLLM). Latency measurements were conducted on an RTX 4090 using vLLM with prefix caching enabled for the BFCL-v3 benchmark evaluation. Accuracy results for FunctionGemma are sourced from its official model card; all other results are obtained from our evaluation.

Preprint. February 2026. <sup>1</sup>Shanghai Jiao Tong University, Shanghai, China <sup>2</sup>Shanghai Innovation Institute, Shanghai, China <sup>3</sup>Fudan University, Shanghai, China. Correspondence to: Xiaoxin Shi <[cialtion737410@sjtu.edu.cn](mailto:cialtion737410@sjtu.edu.cn)>, Zengfeng Huang <[zhuang@fudan.edu.cn](mailto:zhuang@fudan.edu.cn)>.

Preprint. March 3, 2026.

## Abstract

LLM-based function calling enables intelligent agents to interact with external tools and environments, yet autoregressive decoding imposes a fundamental latency bottleneck that limits real-time applications such as embodied intelligence, game AI, and interactive avatars (e.g., 10 Hz con-

control frequency). We observe that function calling differs fundamentally from free-form text generation: structured outputs exhibit substantial token redundancy (delimiters, parameter names), and arguments exhibit weak causal dependencies. Crucially, these two properties must be exploited jointly to achieve real-time performance. We present SimpleTool, which introduces special tokens that serve a dual role: compressing low-entropy tokens ( $4\text{--}6\times$  reduction) while acting as mode selectors that enable independent parallel generation of function name and arguments. This synergistic design achieves  $3\text{--}6\times$  end-to-end speedup (up to  $9.6\times$ ) with only  $+8.2\%$  parallelization overhead. Experiments on five benchmarks across Qwen-series models (0.5B–14B) demonstrate substantial speedup while maintaining competitive or improved accuracy. On Mobile Actions, ST-Qwen-0.5B outperforms Google’s FunctionGemma in both accuracy and latency consistency. With quantization on consumer-grade GPU, SimpleTool achieves 61.2ms P50 latency, enabling 16 Hz real-time control at 4B model scale, bridging the gap between LLM function calling and latency-critical real-world deployment.

## 1. Introduction

Large Language Models (LLMs) have enabled function calling—the mechanism by which LLMs interact with external tools and environments (Brown et al., 2020; O’Neill et al., 2024; Schick et al., 2023). However, a fundamental limitation persists: autoregressive decoding imposes a per-token latency floor that scales linearly with output length (Leviathan et al., 2023; Cai et al., 2024). While streaming masks this latency for conversational applications, function calling requires **complete and valid output before execution**—a partial function call is semantically meaningless. This creates an end-to-end latency bottleneck that streaming cannot alleviate.

### 1.1. The Real-Time Gap

This bottleneck creates a significant gap between LLM capabilities and real-world deployment requirements (Figure 1a).

**Embodied AI & Game AI.** Real-time control demands 5–30 Hz response frequencies. Vision-language-action models like OpenVLA (Kim et al., 2025) achieve only 6 Hz at 166 ms latency (Yu et al., 2025)—far below the sub-100 ms threshold for responsive control. Game AI systems like Lumine (Tan et al., 2025) achieve 5 Hz only through extensive datacenter infrastructure.

**Edge Deployment.** Mobile agents (Yang et al., 2025; Wang

et al., 2024b) rely on cloud APIs with 500 ms–2 s latency per action. Google’s FunctionGemma (Google AI, 2025)—a 270M model for edge function calling—trades capacity for speed, underscoring the need for efficient function calling methods.

### 1.2. Rethinking Acceleration for Function Calling

Function calling end-to-end latency determines the upper bound of LLM-based system capabilities, making acceleration critical. However, existing acceleration methods are not designed for this setting.

**Speculative and Parallel Decoding.** Methods like Medusa (Cai et al., 2024), EAGLE (Li et al., 2024a), and draft-model approaches (Leviathan et al., 2023) accelerate per-token generation through speculation and verification. Though effective for long-form generation, their acceleration benefits are diminished by associated overhead in short-output scenarios such as function calls. We take a more fundamental approach: exploiting the memory-bandwidth bottleneck and idle compute capacity during decoding, combined with the inherent weak causal dependencies in function calling, to enable concurrent decoding of function name and arguments—achieving aggressive end-to-end acceleration. Moreover, these approaches are **orthogonal** to ours and can be combined: we validate this in Appendix J, showing that speculative decoding can achieve up to  $3\times$  additional forward pass reduction with  $>93\%$  token acceptance rate when applied to SimpleTool models.

**Constrained Decoding.** Grammar-guided frameworks like SGLang (Zheng et al., 2024), Outlines (Willard & Louf, 2023), and XGrammar (Dong et al., 2024) ensure output validity and reduce some redundant tokens. Their methods can also reduce end-to-end latency in function calls. However, they remain fundamentally autoregressive, generating tokens sequentially without addressing the core bottleneck: token-by-token decoding.

**Quantization & Compression.** Model compression techniques (Dettmers et al., 2022; Frantar et al., 2023; Lin et al., 2025) provide general acceleration applicable to any task. Our method combines naturally with these approaches (Table 3).

These methods make significant improvements in various aspects. However, they still cannot enable LLMs to make function calls in real time. To achieve this, we advocate a more radical approach that not only leverages parallel decoding but also drastically reduces the number of tokens to be decoded. Furthermore, these two aspects are mutually reinforcing.

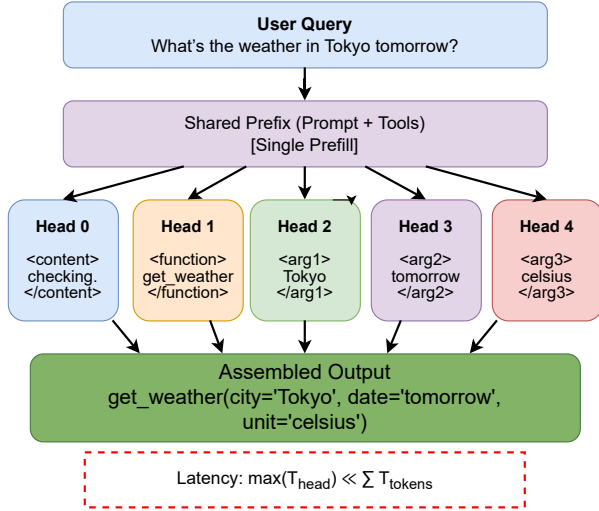


Figure 2. Overview of SimpleTool. Given an input prompt with tool definitions, parallel heads generate function name and arguments independently while sharing the prefix KV cache.

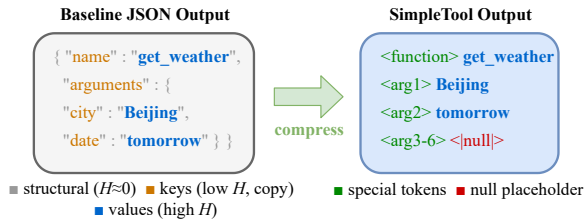


Figure 3. Token compression illustration. Baseline structured output contains  $\sim 30$  tokens spanning three entropy levels. SimpleTool compresses low-entropy tokens into special markers, retaining only high-entropy values for generation.

### 1.3. Key Insight and Our Approach

We observe that function calls generated by LLMs—typically in JSON or Python API format—exhibit two key properties: weak causal dependencies among arguments and substantial token redundancy. Based on this insight, we propose **SimpleTool**, which achieves real-time function calling through two synergistic mechanisms (Figure 2):

**Special Tokens.** We introduce special tokens specifically designed for function calling, which are injected into the vocabulary and can effectively compress redundant tokens. Figure 3 illustrates this mechanism. We demonstrate the effectiveness of special tokens in Table 1: **4–6 $\times$  reduction** compared with vanilla JSON output on samples where both models produce correct outputs. Moreover, these special tokens facilitate parallel decoding as described below.

**Parallel Decoding.** Special tokens further weaken the causal dependencies inherent in function calling, allowing us to treat the function name and its arguments as independent streams. To achieve ultimate speedup, we decode the

function name and arguments in parallel. These parallel streams share the same input prefix and differ only in the appended special token, requiring only a single prefill operation with full reuse of the prefix KV cache. This drastically reduces memory overhead and enables full utilization of idle compute capacity. Consequently, negligible overhead is observed in the time per output token (TPOT) test presented in Appendix G.

### 1.4. Results Overview and Contributions

We conduct comprehensive evaluation on Qwen-series models ranging from 0.5B to 14B parameters across **five benchmarks**: BFCL-v3 (Patil et al., 2025), Mobile Actions (Google AI, 2025), SealTools (Wu et al., 2024), OpenFunction (Patil et al., 2024), and ToolAlpaca (Tang et al., 2023), covering diverse function calling scenarios from API invocation to mobile device control.

Results demonstrate that SimpleTool achieves **3–6 $\times$  speedup** with competitive or improved accuracy across all model sizes and benchmarks. Combined with quantization, our method enables sub-100ms function calling latency with 4B-scale models on consumer-grade GPUs, reaching real-time control frequencies previously infeasible with autoregressive decoding. We additionally compare against Google’s recent model, FunctionGemma (Google AI, 2025), on the Mobile Actions benchmark. In both zero-shot and fine-tuned settings, our smallest model, ST-Qwen2.5-0.5B, demonstrates advantages in both accuracy and latency for edge deployment scenarios.

### Contributions.

- (1) We propose **SimpleTool**, a parallel decoding framework that enables LLMs to call functions in real time, making it possible for LLM-based methods to control real-time interactive systems.
- (2) We design mutually reinforcing special tokens and a parallel decoding architecture that exploits idle compute capacity, conducting an in-depth exploration of redundant token compression and parallel decoding for function calling.
- (3) We train multiple SimpleTool models across the Qwen series (0.5B–14B) and evaluate them on five benchmarks, demonstrating substantial speedup with competitive accuracy.
- (4) We compare against Google’s FunctionGemma on Mobile Actions in both zero-shot and fine-tuned settings, showing more effective edge deployment capability.

Table 1. Token compression ratio across model sizes. CR = Base-line tokens / SimpleTool bottleneck-head tokens. Statistics computed on samples where both models produce correct outputs. Per-benchmark breakdown in Appendix H.

Model	CR (Mean)	CR (P50)	CR (P90)
Qwen2.5-0.5B	5.06×	6.00×	4.06×
Qwen2.5-1.5B	4.32×	4.71×	3.20×
Qwen2.5-3B	4.38×	4.71×	3.20×
Qwen3-4B	4.32×	4.86×	3.42×
Qwen2.5-7B	5.35×	5.00×	3.40×
Qwen2.5-14B	4.51×	4.86×	3.47×
<b>Average</b>	<b>4.66×</b>	<b>5.02×</b>	<b>3.46×</b>

## 2. Methodology

Building on the insight that function calling exhibits structural redundancy and weak causal dependencies (Section 1), this section presents the technical realization of SimpleTool. The key challenge is that these two properties must be exploited *jointly*: compressing redundant tokens alone does not break sequential decoding, while parallelizing without compression leaves substantial latency unreduced.

We describe how special tokens and parallel decoding work synergistically: special tokens not only compress output length (4–6× reduction) but also serve as **mode selectors** that enable independent generation of function name and arguments (Section 2.1). The training strategy then ensures the model learns to leverage both mechanisms effectively (Section 2.2).

### 2.1. Special Tokens Enable Parallel Decoding

#### 2.1.1. FROM REDUNDANCY TO COMPRESSION

Intuitively, conventional function call outputs contain three token categories with distinct entropy characteristics. (Figure 3):

- **Structural tokens** (`{`, `}`, `:`, `,`, `;`): Fully predictable given the output format, near-zero entropy.
- **Key tokens** (“name”, “arguments”, parameter names): Copied from tool definitions, low entropy.
- **Value tokens** (function names, argument values): Require actual LLM reasoning, high entropy.

We introduce special tokens (`<function>`, `<arg1>`–`<arg6>` e.g.) that absorb all low-entropy information, achieving 4–6× compression (Table 1). Crucially, these tokens serve a dual purpose: beyond compression, each token acts as a **mode selector**, signaling which component (function name, specific argument or even content) to generate. This dual role—compression *and* mode selection—is what enables parallel decoding.

#### 2.1.2. FROM WEAK DEPENDENCIES TO PARALLEL DECODING

With special tokens serving as mode selectors, we can exploit the weak causal dependencies among function arguments: since each argument can be inferred largely independently from the input context, we decode them as **parallel streams** rather than sequentially.

**Architecture.** As illustrated in Figure 2, SimpleTool decouples function calling into  $H$  independent decoding streams (1 for function name, up to 6 for arguments, more if needed in training), each initialized by appending a distinct special token (`<function>`, `<arg1>`, ..., `<arg6>`) to the shared input prefix. We also reserve a content head (`<content>`) for chatting, which can be optionally used alongside function calls. All streams share the same prefix KV cache; only the head-specific special token differs. This design directly leverages the dual role of special tokens: they compress the output *and* specify which component to generate.

**Latency Analysis.** For conventional autoregressive decoding, end-to-end latency is:

$$T_{\text{baseline}} = T_p + N \cdot T_d \quad (1)$$

where  $T_p$  is prefill time,  $N$  is total output tokens, and  $T_d$  is per-token decode latency. With SimpleTool, the latency becomes:

$$T_{\text{ours}} \approx T_p + \max_{i \in \{1, \dots, H\}} (N_i) \cdot T_d \quad (2)$$

where  $H$  is the number of parallel decoding heads,  $N_i$  is the token count for head  $i$ , and some insignificant overhead may exist. End-to-end latency is thus dominated by the **longest single head**, not the sum of all heads.

#### 2.1.3. PARALLEL DECODING AS A NEAR-FREE OPERATION

One might expect  $H$  parallel decoding streams to incur proportional computational overhead. We argue—and empirically validate—that this cost is negligible due to the **memory-bandwidth-bound** nature of autoregressive decoding.

During the decode phase, each token generation requires loading the full model weights from GPU memory, while the actual computation (a single matrix-vector product per layer) utilizes only a fraction of available FLOPS. This creates substantial idle compute capacity. Batching multiple sequences—in our case, parallel heads within the same request—increases arithmetic intensity without proportionally increasing memory traffic, effectively utilizing otherwise-idle compute.

We validate this through batch scaling experiments (shown in Appendix G). Across six model configurations from 0.5B

to 14B parameters with the same prefix and one different token, 8-head parallel decoding achieves **93.0% average TPOT efficiency**, with efficiency only dropping markedly at extremely large batch sizes, demonstrating that SimpleTool’s parallel heads operate well within the memory-bound bottleneck and idle compute capacity.

**KV Cache Efficiency.** All parallel heads share the input prefix, enabling full KV cache reuse. For an input of  $L$  tokens and  $H$  heads each appending a single special token, the KV cache overhead is only  $H$  tokens beyond the shared prefix—negligible compared to typical prompt lengths. In high-frequency control scenarios where the tool schema remains fixed, this shared prefix can be persistently cached, further amortizing prefill cost (see Section 3.4 for empirical validation).

## 2.2. Training for Parallel Generation

The synergistic design described above requires the model to learn a fundamentally different output behavior: generating function name and arguments as **independent streams** conditioned on distinct special tokens, while maintaining reasoning capability.

### 2.2.1. SPECIAL TOKEN DESIGN

We introduce 17 special tokens organized into four functional groups:

**Content head:** `<content>`, `</content>` for natural language responses.

**Function head:** `<function>`, `</function>` for function name generation.

**Argument heads:** `<arg $k$ >`, `</arg $k$ >` for  $k \in \{1, \dots, 6\}$ , each selecting a positional argument.

**Placeholder:** `<|null|>` for unused argument slots, enabling early termination of inactive heads.

Each special token encodes all structural information (delimiters, parameter names, positional ordering) into its semantics, eliminating the need to generate them explicitly while simultaneously specifying the generation mode.

### 2.2.2. TRAINING CHALLENGES

Achieving high-quality parallel decoding is non-trivial. Unlike standard fine-tuning where the model learns a single output distribution, SimpleTool requires the model to learn **eight distinct output modes** that share the same input but produce semantically different outputs. This poses two key challenges:

**Capacity Requirements.** Learning multiple output modes demands sufficient model plasticity. We find that standard LoRA configurations underperform for this task; significantly larger adapter capacity is required to capture the

diverse output patterns without interference between heads (see ablation in Section 3.5). Moreover, the introduction of special tokens necessitates unfreezing the embedding layer—a departure from standard parameter-efficient fine-tuning that requires careful optimization to balance learning new token representations against preserving pretrained knowledge.

**Data Distribution Balance.** Existing function calling datasets exhibit skewed argument count distributions, with most samples concentrated around 2–3 arguments. For SimpleTool’s multi-head architecture, underrepresented argument counts (0, 5, 6 arguments) lead to poorly trained heads that fail to generalize. We address this through targeted data augmentation using synthetic samples that balance argument count distribution (see ablation in Section 3.5).

### 2.2.3. TRAINING PIPELINE

We adopt parameter-efficient fine-tuning with LoRA (Hu et al., 2022), targeting the MLP layers to maximize the capacity for learning head-specific output patterns. Training samples are formatted as parallel sequences sharing identical prefixes but differing in the appended special token and corresponding target output. The loss is computed independently for each head with head-specific weighting to address output length imbalance. Hyperparameter details are provided in Appendix F.

## 3. Experiments

We evaluate SimpleTool from four perspectives: (1) **accuracy** on multiple benchmarks (Section 3.2), (2) **inference speedup** (Section 3.3), (3) **domain adaptation** comparing with FunctionGemma (Section 3.4), and (4) **ablation studies** (Section 3.5).

### 3.1. Experimental Setup

**Models.** We evaluate on Qwen2.5-Instruct series (0.5B–14B) (Qwen Team, 2024) and Qwen3-4B-Instruct (Yang et al., 2025). All models are fine-tuned using LoRA (Hu et al., 2022) with a relatively large rank (we explore this setting in Section 3.5). We set the number of parallel argument heads to 6, which already covers **95.2%** of function calls across all evaluation benchmarks (see Appendix C for detailed statistics).

**Benchmarks.** We evaluate on five benchmarks covering diverse function calling scenarios: BFCL-v3 (Patil et al., 2024) (single-turn subsets), Mobile Actions (Google AI, 2025), SealTools (Wu et al., 2024), OpenFunction-v1 (Patil et al., 2024), and ToolAlpaca (Tang et al., 2023). The last three benchmarks are combined into an “Others” group for aggregate evaluation.

**Metrics.** Overall Accuracy (complete correctness including function name and all arguments) and Function Accuracy (function name selection only).

**Hardware.** Inference latency is measured on RTX 4090 and H100 GPUs.

### 3.2. Accuracy Evaluation

Table 2 and Figure 4 present comprehensive accuracy evaluation across model scales and benchmarks.

**Consistent improvement across model scales.** All model sizes show overall accuracy gains ranging from +0.5% (1.5B) to +3.5% (7B), with an average improvement of +2.9%. This consistency suggests that models have learned these new output modes effectively.

**Substantial function accuracy gains.** Average function accuracy increases +7.1% over baselines, with several configurations achieving near-perfect scores. We attribute this to special tokens acting as mode selectors: by explicitly conditioning each head on its target component, the model avoids ambiguity in output structure. Additionally, the compressed output format means fewer tokens and thus fewer opportunities for errors—particularly important in function calling where a single incorrect token invalidates the entire output.

**Strongest gains on Mobile Actions.** Improvements range from +7.3% to +13.3% across model sizes. Notably, this benchmark was released in December 2025 (Google AI, 2025), after both baseline models and our training data were finalized, demonstrating strong generalization to unseen domains.

### 3.3. Speedup Evaluation

Figure 5 presents speedup evaluation in different settings, demonstrating the effectiveness of SimpleTool’s acceleration strategies.

**Basic Parallelization** (Figure 5a): With the Transformers backend, SimpleTool achieves 2.8–5.4× speedup on RTX 4090 and 3.0–6.4× on H100. Smaller models benefit more due to their decode-bound characteristics.

**Prefix Caching** (Figure 5b): vLLM’s KV cache sharing across parallel streams yields 2.7–4.4× speedup, with larger models showing improved ratios as prefix caching amortizes shared computation more effectively.

**Quantization** (Figure 5c): AWQ 4-bit quantization achieves the lowest absolute latency. Qwen3-4B reaches **61.2ms** P50, corresponding to 16 Hz control frequency—exceeding the 10 Hz threshold typically required for real-time applications.

**Parallelization Overhead** (Figure 5d): As active heads increase from 2 to 8, speedup remains stable, confirming

that parallelization overhead is negligible—consistent with our analysis that parallel streams utilize otherwise-idle compute capacity within the memory-bandwidth-bound decode phase. Note that Figure 5d reflects end-to-end measurements where varying output lengths across heads introduce additional variance; controlled experiments isolating batch size effects are provided in Appendix G.

Table 3 summarizes results across the acceleration hierarchy. Models up to 7B achieve sub-100ms latency on consumer-grade RTX 4090, enabling real-time deployment without datacenter infrastructure.

### 3.4. Case Study: Comparison with FunctionGemma

We compare against FunctionGemma (Google AI, 2025), Google’s 270M model released in December 2025 specifically for edge function calling, to evaluate whether SimpleTool can compete with industry solutions designed for on-device deployment.

**Setup.** We evaluate on the Mobile Actions dataset released alongside FunctionGemma, containing ~9,600 samples covering 7 smartphone operations. This benchmark complements BFCL-v3 by focusing on mobile device control—a scenario closely aligned with our target real-time applications. For domain adaptation, we fine-tune ST-Qwen-0.5B on the official training split using LoRA ( $r = 64$ ), requiring less than 3 H100-hours. Latency is measured on the full test split (1,283 samples) using vLLM with prefix caching.

**Results** (Tables 4–5): ST-Qwen-0.5B achieves 69.3% zero-shot (+11.3% vs FunctionGemma) and 86.2% after fine-tuning, surpassing both FunctionGemma (85.0%) and the 8× larger Qwen3-4B (83.7%). Despite 1.8× more parameters, ST-Qwen-0.5B achieves faster inference (51.0ms vs 61.1ms P50) with substantially better tail latency (74.5ms vs 139.5ms P90)—critical for real-time applications where worst-case latency determines reliability.

### 3.5. Ablation Studies

We conduct ablation studies on Qwen3-4B evaluated on BFCL-v3 (Table 6).

**LoRA Rank.** Performance improves with larger ranks, reaching 87.0% at rank 1024, suggesting that learning eight distinct output modes benefits from increased adapter capacity. We adopt rank 512 as default.

**Training Data.** Using only public xLAM data (Zhang et al., 2025), SimpleTool achieves 85.3%—demonstrating strong performance without proprietary data. Synthetic augmentation via Qwen3-235B yields +1.0% improvement.

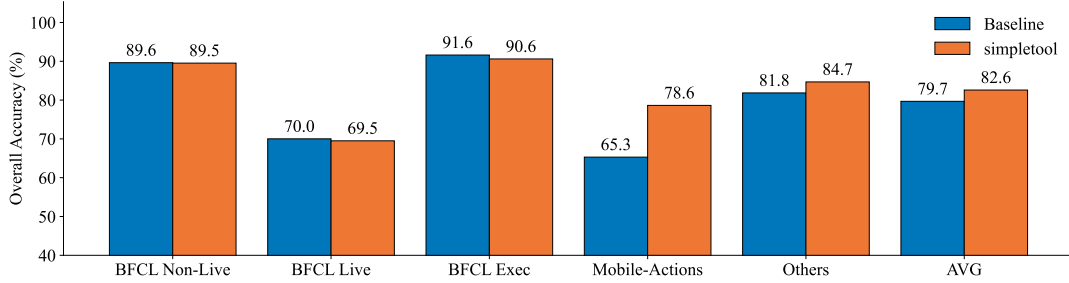


Figure 4. Average accuracy comparison between Baseline and SimpleTool across benchmark groups (macro average). BFCL-v3 is evaluated on single-turn subsets; Mobile Actions parallel calls are converted to multi-turn format; “Others” combines SealTools, OpenFunc, and ToolAlpaca.

Table 2. Performance comparison on five benchmarks. Each cell shows overall (function) accuracy, e.g., 78.3 (98.3). Speedup ratio after model name indicates inference acceleration on RTX 4090 with vLLM (P50 latency). **Bold** = best, underline = second best within each column (applied separately to overall and function accuracy).

Model	BFCL Non-Live	BFCL Live	BFCL Exec	Mobile Actions	Others	AVG
<i>Baseline Models</i>						
Qwen2.5-0.5B (1×)	78.3 (98.3)	49.9 (86.4)	88.6 (96.6)	56.7 (74.4)	80.9 (95.2)	70.9 (90.2)
Qwen2.5-1.5B (1×)	86.3 (98.3)	67.4 (90.4)	91.9 (98.0)	65.5 (74.9)	82.2 (95.3)	78.7 (91.4)
Qwen2.5-3B (1×)	92.5 (99.7)	73.0 (94.3)	86.6 (96.0)	66.2 (75.0)	84.3 (95.9)	80.5 (92.2)
Qwen3-4B (1×)	<u>93.7</u> (99.3)	<b>77.9</b> (94.5)	<b>94.6</b> (97.3)	68.0 (75.0)	82.0 (91.8)	83.2 (91.6)
Qwen2.5-7B (1×)	93.0 (99.7)	75.4 (95.2)	<u>94.0</u> (99.3)	68.4 (77.2)	83.4 (94.9)	82.8 (93.3)
Qwen2.5-14B (1×)	<b>94.0</b> (99.3)	<u>76.6</u> (95.9)	<u>94.0</u> (98.7)	67.0 (75.0)	78.3 (89.5)	82.0 (91.7)
<i>SimpleTool (Ours)</i>						
ST-Qwen2.5-0.5B (3.1×)	79.8 ( <b>99.8</b> )	57.2 (91.6)	87.9 ( <b>100.0</b> )	69.3 (99.3)	82.2 (99.1)	75.3 (98.0)
ST-Qwen2.5-1.5B (3.5×)	88.8 ( <b>99.8</b> )	63.6 (94.3)	90.6 ( <b>100.0</b> )	72.8 ( <b>100.0</b> )	80.2 (99.3)	79.2 (98.7)
ST-Qwen2.5-3B (3.8×)	90.3 ( <b>99.8</b> )	68.0 (95.4)	91.3 ( <b>100.0</b> )	81.4 ( <u>99.9</u> )	85.5 ( <u>99.5</u> )	83.3 (98.9)
ST-Qwen3-4B (3.9×)	92.5 (99.5)	76.4 (96.3)	89.9 ( <b>100.0</b> )	<b>84.5</b> (99.9)	86.6 ( <b>99.7</b> )	86.0 (99.1)
ST-Qwen2.5-7B (4.5×)	93.5 ( <b>99.8</b> )	75.8 (96.7)	92.6 ( <b>100.0</b> )	<u>83.2</u> ( <b>100.0</b> )	86.2 ( <u>99.5</u> )	<b>86.3</b> (99.2)
ST-Qwen2.5-14B (4.4×)	92.2 (99.7)	75.9 ( <b>97.1</b> )	91.3 ( <b>100.0</b> )	80.5 ( <b>100.0</b> )	<b>87.4</b> (99.7)	85.5 ( <b>99.3</b> )

Table 3. Speedup and latency summary on RTX 4090.

Model	Trans.	vLLM	AWQ (ms)
Qwen2.5-0.5B	5.35×	3.07×	32.1
Qwen2.5-1.5B	3.32×	3.46×	39.4
Qwen2.5-3B	2.93×	3.78×	53.9
Qwen3-4B	2.83×	3.88×	61.2
Qwen2.5-7B	–	–	89.3
Qwen2.5-14B	–	–	142.5

## 4. Limitations

**Argument Independence.** SimpleTool assumes function arguments can be generated independently—valid for well-designed APIs with unordered key-value parameters. When semantic dependencies exist (e.g., `file.path` and `line.number`), dependent parameters can be consolidated into a single head, trading parallelism for correctness.

**Fixed Head Count.** The 6-argument head configuration covers 95.2% of functions in our benchmarks. APIs exceeding this limit can concatenate overflow parameters into the final head, preserving functionality with reduced paral-

Table 4. Accuracy on Mobile Actions.

Model	Zero-shot	Fine-tuned
Qwen3-4B-Instruct	83.7	–
FunctionGemma (270M)	58.0	85.0
ST-Qwen-0.5B (Ours)	<b>69.3</b>	<b>86.2</b>
Δ vs FunctionGemma	+11.3	+1.2

Table 5. Latency on Mobile Actions (vLLM, RTX 4090).

Model	P50 (ms)	P90 (ms)	Speedup
Qwen3-4B (Baseline)	468.5	667.0	1.0×
Qwen2.5-0.5B (Baseline)	110.1	154.0	4.3×
FunctionGemma (270M)	61.1	139.5	7.7×
<b>ST-Qwen-0.5B (Ours)</b>	<b>51.0</b>	<b>74.5</b>	<b>9.2×</b>

lelism.

**Training Cost.** Processing each head as an independent sequence incurs computational overhead compared to standard fine-tuning, acceptable for one-time model preparation but limiting rapid iteration.

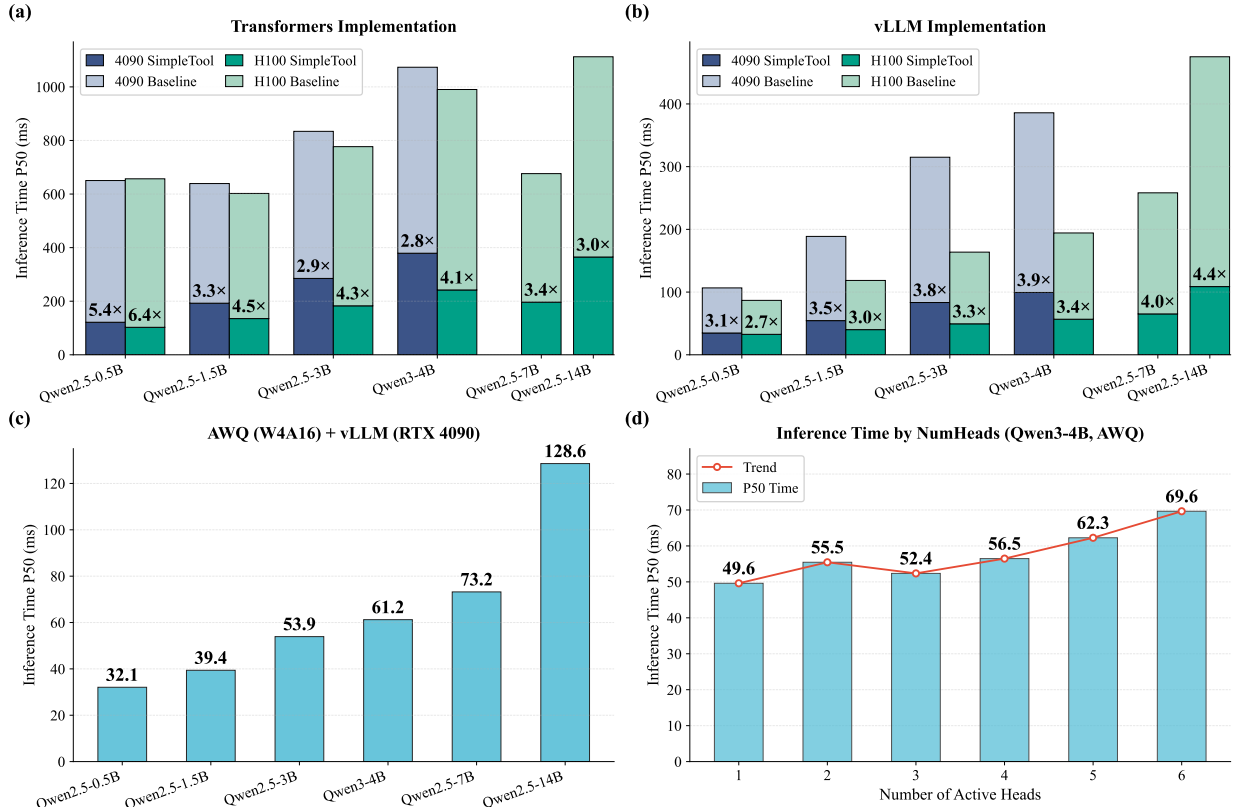


Figure 5. **Inference speedup evaluation.** (a)–(b) Stacked bars show baseline time partitioned into SimpleTool time (dark) and time saved (light); speedup ratios labeled at boundary. (a) Transformers backend on RTX 4090 (blue) and H100 (green). (b) vLLM backend with prefix caching. (c) Absolute latency with AWQ quantization on RTX 4090. (d) Latency scaling with number of active heads (Qwen3-4B, AWQ in 4090). All measurements on BFCL-v3 single-turn cases.

Table 6. Ablation studies on BFCL-v3 (Qwen3-4B).

LoRA Rank	Acc. (%)	Training Data	Acc. (%)
64	85.5	xLAM only (public)	85.3
256	86.4	xLAM + Synthetic	<b>86.3</b>
512	85.3		
1024	<b>87.0</b>		

## 5. Future Work

**Open Source and Real-World Deployment.** We plan to release training code and model weights to facilitate adoption in latency-critical applications: robotic control systems requiring sub-100ms actions, real-time avatars, and interactive coding assistants.

**Vision-Language Extension.** Extending SimpleTool to VLMs would enable real-time Vision-Language-Action systems for embodied AI, with the key challenge being efficient visual token handling while maintaining parallel action decoding.

**On-Device Deployment.** Bridging server-side speedup to edge deployment requires optimization for mobile frameworks (LiteRT, Core ML, ExecuTorch) and adapting parallel

decoding to device constraints.

**Adaptive Heads.** Dynamically adjusting active head count based on tool schemas at inference time would improve flexibility for diverse APIs.

**Scaling.** Investigating behavior on 30B+ models remains important—whether accuracy gains persist at scale or stronger baselines reduce the relative benefit.

## 6. Conclusion

We presented SimpleTool, a parallel decoding framework for real-time LLM function calling. Our key insight is that structured function outputs exhibit structural redundancy and weak causal dependencies among arguments—two properties that must be exploited jointly. We introduced special tokens that serve a dual role: compressing predictable tokens (4–6× reduction) while acting as mode selectors that enable independent generation of function name and arguments. This synergistic design allows parallel decoding streams to share the prefix KV cache with negligible overhead, achieving 3–6× end-to-end speedup while maintaining competitive accuracy across five benchmarks.

Combined with quantization, SimpleTool enables 4B-scale models to achieve 16+ Hz real-time function calling on consumer GPUs, bridging the gap between LLM capabilities and latency-critical applications such as embodied AI, game AI, and interactive agents.

## Impact Statement

This paper advances real-time LLM function calling, enabling latency-critical applications such as embodied AI, game AI, and interactive agents. We foresee positive societal impacts including more responsive assistive robotics, accessible AI tutoring systems, and democratized deployment of capable AI on consumer hardware.

Potential risks include misuse in autonomous systems operating without adequate human oversight. We recommend that practitioners deploying SimpleTool in safety-critical domains implement appropriate safeguards, monitoring mechanisms, and human-in-the-loop controls. The authors have no conflicts of interest to disclose.

## References

- Ankner, Z., Parthasarathy, R., Nrusimha, A., Rinard, C., Ragan-Kelley, J., and Brandon, W. Hydra: Sequentially-dependent draft heads for Medusa decoding. *CoRR*, 2024.
- Black, K., Brown, N., Driess, D., et al.  $\pi_0$ : A vision-language-action flow model for general robot control. *arXiv preprint arXiv:2410.24164*, 2024.
- Brown, T., Mann, B., Ryder, N., Subbiah, M., Kaplan, J. D., Dhariwal, P., Neelakantan, A., Shyam, P., Sastry, G., Askell, A., et al. Language models are few-shot learners. *Advances in Neural Information Processing Systems*, 33: 1877–1901, 2020.
- Cai, T., Li, Y., Geng, Z., Peng, H., Lee, J. D., Chen, D., and Dao, T. Medusa: Simple LLM inference acceleration framework with multiple decoding heads. In *International Conference on Machine Learning*, pp. 5209–5235. PMLR, 2024.
- Chen, C., Borgeaud, S., Irving, G., Lespiau, J.-B., Sifre, L., and Jumper, J. Accelerating large language model decoding with speculative sampling. *arXiv preprint arXiv:2302.01318*, 2023.
- Dettmers, T., Lewis, M., Belkada, Y., and Zettlemoyer, L. GPT3.int8(): 8-bit matrix multiplication for transformers at scale. *Advances in Neural Information Processing Systems*, 35:30318–30332, 2022.
- Dong, Y., Ruan, C. F., Cai, Y., Lai, R., Xu, Z., Zhao, Y., and Chen, T. XGrammar: Flexible and efficient structured generation engine for large language models. *Proceedings of Machine Learning and Systems 7*, 2024.
- Frantar, E., Ashkboos, S., Hoefler, T., and Alistarh, D. GPTQ: Accurate post-training quantization for generative pre-trained transformers. In *International Conference on Learning Representations (ICLR)*, 2023.
- Gim, I., Lee, S.-s., and Zhong, L. Asynchronous llm function calling. *arXiv preprint arXiv:2412.07017*, 2024.
- Gloeckle, F., Idrissi, B. Y., Rozière, B., Lopez-Paz, D., and Synnaeve, G. Better & faster large language models via multi-token prediction. In *Proceedings of the 41st International Conference on Machine Learning*, pp. 15706–15734, 2024.
- Gong, J., Huang, Y., Yuan, B., Zhu, M., Liao, Z., Liang, J., Zhan, J., Wang, J., Shu, H., Xiong, M., et al. Ghostshell: Streaming llm function calls for concurrent embodied programming. *arXiv preprint arXiv:2508.05298*, 2025.
- Google AI. FunctionGemma: Bringing bespoke function calling to the edge. <https://blog.google/technology/developers/functiongemma/>, December 2025. Accessed: 2026-01-07.
- Guo, Z., Cheng, S., Wang, H., Liang, S., Qin, Y., Li, P., Liu, Z., Sun, M., and Liu, Y. StableToolBench: Towards stable large-scale benchmarking on tool learning of large language models. In *Findings of the Association for Computational Linguistics: ACL 2024*, pp. 11143–11156, Bangkok, Thailand, 2024. Association for Computational Linguistics. doi: 10.18653/v1/2024.findings-acl.664. URL <https://aclanthology.org/2024.findings-acl.664/>.
- Hu, E. J., Shen, Y., Wallis, P., Allen-Zhu, Z., Li, Y., Wang, S., Wang, L., and Chen, W. LoRA: Low-rank adaptation of large language models. In *International Conference on Learning Representations*, 2022. URL <https://openreview.net/forum?id=nZeVKeeFYf9>.
- Kim, M. J., Pertsch, K., Karamcheti, S., Xiao, T., Balakrishna, A., Nair, S., Rafailov, R., Foster, E. P., Sanketi, P. R., Vuong, Q., et al. OpenVLA: An open-source vision-language-action model. In *Conference on Robot Learning*, pp. 2679–2713. PMLR, 2025.
- Kim, S., Moon, S., Tabrizi, R., Lee, N., Mahoney, M. W., Keutzer, K., and Gholami, A. An llm compiler for parallel function calling. In *International Conference on Machine Learning*, pp. 24370–24391. PMLR, 2024.
- Kwon, W., Li, Z., Zhuang, S., Sheng, Y., Zheng, L., Yu, C. H., Gonzalez, J., Zhang, H., and Stoica, I. Efficient memory management for large language model serving

- with PagedAttention. In *Proceedings of the 29th Symposium on Operating Systems Principles*, pp. 611–626, 2023.
- Leviathan, Y., Kalman, M., and Matias, Y. Fast inference from transformers via speculative decoding. In *International Conference on Machine Learning*, pp. 19274–19286. PMLR, 2023.
- Li, Y., Wei, F., Zhang, C., and Zhang, H. EAGLE: Speculative sampling requires rethinking feature uncertainty. In *International Conference on Machine Learning*, 2024a.
- Li, Y., Wei, F., Zhang, C., and Zhang, H. EAGLE-2: Faster inference of language models with dynamic draft trees. In *Empirical Methods in Natural Language Processing*, 2024b.
- Li, Y., Wei, F., Zhang, C., and Zhang, H. EAGLE-3: Scaling up inference acceleration of large language models via training-time test. In *Annual Conference on Neural Information Processing Systems*, 2025.
- Lin, J., Tang, J., Tang, H., Yang, S., Xiao, G., and Han, S. AWQ: Activation-aware weight quantization for on-device LLM compression and acceleration. *GetMobile: Mobile Computing and Communications*, 28(4):12–17, 2025.
- Ning, X., Lin, Z., Zhou, Z., Wang, Z., Yang, H., and Wang, Y. Skeleton-of-thought: Prompting LLMs for efficient parallel generation. In *The Twelfth International Conference on Learning Representations*, 2024. URL <https://openreview.net/forum?id=mqVgBbNCm9>.
- O’Neill, A., Rehman, A., Maddukuri, A., Gupta, A., Padalkar, A., Lee, A., Pooley, A., Gupta, A., Mandlekar, A., Jain, A., et al. Open X-Embodiment: Robotic learning datasets and RT-X models: Open X-Embodiment collaboration0. In *2024 IEEE International Conference on Robotics and Automation, ICRA 2024*, pp. 6892–6903. Institute of Electrical and Electronics Engineers Inc., 2024.
- Patil, S. G., Zhang, T., Wang, X., and Gonzalez, J. E. Gorilla: Large language model connected with massive APIs. *Advances in Neural Information Processing Systems*, 37: 126544–126565, 2024.
- Patil, S. G., Mao, H., Yan, F., Ji, C. C.-J., Suresh, V., Stoica, I., and Gonzalez, J. E. The berkeley function calling leaderboard (BFCL): From tool use to agentic evaluation of large language models. In *Forty-second International Conference on Machine Learning*, 2025. URL <https://openreview.net/forum?id=2GmDdhBdDk>.
- Qin, Y., Liang, S., Ye, Y., Zhu, K., Yan, L., Lu, Y., Lin, Y., Cong, X., Tang, X., Qian, B., Zhao, S., Hong, L., Tian, R., Xie, R., Zhou, J., Gerstein, M., Li, D., Liu, Z., and Sun, M. ToolLLM: Facilitating large language models to master 16000+ real-world APIs. In *The Twelfth International Conference on Learning Representations*, 2024. URL <https://openreview.net/forum?id=dHng200Jjr>.
- Qwen Team. Qwen2.5: A party of foundation models, September 2024. URL <https://qwenlm.github.io/blog/qwen2.5/>.
- Schick, T., Dwivedi-Yu, J., Dessi, R., Raileanu, R., Lomeli, M., Hambro, E., Zettlemoyer, L., Cancedda, N., and Scialom, T. Toolformer: Language models can teach themselves to use tools. *Advances in Neural Information Processing Systems*, 36:68539–68551, 2023.
- SIMA Team, Raad, M. A., Ahuja, A., Barros, C., Besse, F., Bolt, A., Bolton, A., Brownfield, B., Buttimore, G., Cant, M., Chakera, S., Chan, S. C. Y., Clune, J., Collister, A., Copeman, V., Cullum, A., Dasgupta, I., de Cesare, D., Di Trapani, J., Donchev, Y., Dunleavy, E., Engelcke, M., Faulkner, R., Garcia, F., Gbadamosi, C., Gong, Z., Gonzales, L., Gupta, K., Gregor, K., Hallingstad, A. O., Harley, T., Haves, S., Hill, F., Hirst, E., Hudson, D. A., Hudson, J., Hughes-Fitt, S., Rezende, D. J., Jasarevic, M., Kamps, L., Ke, R., Keck, T., Kim, J., Knagg, O., Koppurapu, K., Lampinen, A., Legg, S., Lerchner, A., Limont, M., Liu, Y., Loks-Thompson, M., Marino, J., Cussons, K. M., Matthey, L., McLoughlin, S., Mendolicchio, P., Merzic, H., Mitenkova, A., Moufarek, A., Oliveira, V., Oliveira, Y., Openshaw, H., Pan, R., Pappu, A., Platonov, A., Purkiss, O., Reichert, D., Reid, J., Richemond, P. H., Roberts, T., Ruscoe, G., Elias, J. S., Sandars, T., Sawyer, D. P., Scholtes, T., Simmons, G., Slater, D., Soyer, H., Strathmann, H., Stys, P., Tam, A. C., Teplyashin, D., Terzi, T., Vercelli, D., Vujatovic, B., Wainwright, M., Wang, J. X., Wang, Z., Wierstra, D., Williams, D., Wong, N., York, S., and Young, N. Scaling instructable agents across many simulated worlds, 2024.
- Tan, W., Li, X., Fang, Y., Yao, H., Yan, S., Luo, H., Ao, T., Li, H., Ren, H., Yi, B., et al. Lumine: An open recipe for building generalist agents in 3D open worlds. *arXiv preprint arXiv:2511.08892*, 2025.
- Tang, Q., Deng, Z., Lin, H., Han, X., Liang, Q., and Sun, L. ToolAlpaca: Generalized tool learning for language models with 3000 simulated cases, 2023.
- Wang, G., Xie, Y., Jiang, Y., Mandlekar, A., Xiao, C., Zhu, Y., Fan, L., and Anandkumar, A. Voyager: An open-ended embodied agent with large language models. *Transactions on Machine Learning Research*, 2024a. ISSN 2835-8856. URL <https://openreview.net/forum?id=ehfRiF0R3a>.

- Wang, J., Xu, H., Ye, J., Yan, M., Shen, W., Zhang, J., Huang, F., and Sang, J. Mobile-agent: Autonomous multi-modal mobile device agent with visual perception. *CoRR*, 2024b.
- Wen, H., Li, Y., Liu, G., Zhao, S., Yu, T., Li, T. J.-J., Jiang, S., Liu, Y., Zhang, Y., and Liu, Y. AutoDroid: LLM-powered task automation in Android. In *Proceedings of the 30th Annual International Conference on Mobile Computing and Networking*, pp. 543–557, 2024.
- Willard, B. T. and Louf, R. Efficient guided generation for large language models. *arXiv preprint arXiv:2307.09702*, 2023.
- Wu, M., Zhu, T., Han, H., Tan, C., Zhang, X., and Chen, W. SEAL-Tools: Self-instruct tool learning dataset for agent tuning and detailed benchmark. In *CCF International Conference on Natural Language Processing and Chinese Computing*, pp. 372–384. Springer, 2024.
- Xia, H., Yang, Z., Dong, Q., Wang, P., Li, Y., Ge, T., Liu, T., Li, W., and Sui, Z. Unlocking efficiency in large language model inference: A comprehensive survey of speculative decoding. In *Findings of the Association for Computational Linguistics: ACL 2024*, pp. 7655–7671, Bangkok, Thailand, 2024. Association for Computational Linguistics. doi: 10.18653/v1/2024.findings-acl.456. URL <https://aclanthology.org/2024.findings-acl.456/>.
- Yang, A., Li, A., Yang, B., Zhang, B., Hui, B., Zheng, B., Yu, B., Gao, C., Huang, C., Lv, C., et al. Qwen3 technical report. *arXiv preprint arXiv:2505.09388*, 2025.
- Yang, N., Ge, T., Wang, L., Jiao, B., Jiang, D., Yang, L., Majumder, R., and Wei, F. Inference with reference: Lossless acceleration of large language models. *arXiv preprint arXiv:2304.04487*, 2023.
- Yu, Z., Wang, B., Zeng, P., Zhang, H., Zhang, J., Gao, L., Song, J., Sebe, N., and Shen, H. T. A survey on efficient vision-language-action models. *arXiv preprint arXiv:2510.24795*, 2025.
- Zhang, J., Lan, T., Zhu, M., Liu, Z., Hoang, T. Q., Kokane, S., Yao, W., Tan, J., Prabhakar, A., Chen, H., et al. xLAM: A family of large action models to empower AI agent systems. In *Proceedings of the 2025 Conference of the Nations of the Americas Chapter of the Association for Computational Linguistics: Human Language Technologies (Volume 1: Long Papers)*, pp. 11583–11597, 2025.
- Zheng, L., Yin, L., Xie, Z., Sun, C. L., Huang, J., Yu, C. H., Cao, S., Kozyrakis, C., Stoica, I., Gonzalez, J. E., et al. SGLang: Efficient execution of structured language model programs. *Advances in Neural Information Processing Systems*, 37:62557–62583, 2024.
- Zitkovich, B., Yu, T., Xu, S., Xu, P., Xiao, T., Xia, F., Wu, J., Wohlhart, P., Welker, S., Wahid, A., et al. RT-2: Vision-language-action models transfer web knowledge to robotic control. In *Conference on Robot Learning*, pp. 2165–2183. PMLR, 2023.

## A. Other Related Work

**LLM Function Calling and Tool Use.** The ability of LLMs to interact with external tools has been extensively studied. Toolformer (Schick et al., 2023) explored self-supervised tool learning, while Gorilla (Patil et al., 2024) and ToolLLM (Qin et al., 2024) improved accuracy through retrieval-augmented approaches. xLAM (Zhang et al., 2025) addresses function calling through data augmentation strategies. At the orchestration level, several works explore parallelism and scheduling: LLM Compiler (Kim et al., 2024) investigates parallel function calling, Skeleton-of-Thought (Ning et al., 2024) explores parallel generation via prompting strategies, AsyncLM (Gim et al., 2024) proposes asynchronous execution patterns, and GhostShell (Gong et al., 2025) addresses concurrent tool execution in embodied settings. LLMA (Yang et al., 2023) explores reference-based acceleration techniques. For evaluation, BFCL (Patil et al., 2024) and StableToolBench (Guo et al., 2024) provide standardized benchmarks, while Mobile Actions (Google AI, 2025) targets edge deployment scenarios. Google’s FunctionGemma (Google AI, 2025) represents industry efforts toward compact, edge-deployable models.

**Speculative and Parallel Decoding.** Speculative decoding (Leviathan et al., 2023; Chen et al., 2023) accelerates inference using draft-and-verify mechanisms. Medusa (Cai et al., 2024) and the EAGLE series (Li et al., 2024a;b; 2025) introduce parallel decoding heads, while Hydra (Ankner et al., 2024) explores sequentially-dependent draft heads. Multi-token prediction (Gloeckle et al., 2024) trains models to predict multiple future tokens. A comprehensive survey is provided by Xia et al. (2024). Unlike these general-purpose methods, SimpleTool exploits the structural properties of function calling, achieving parallelism without additional parameters or draft models.

**Structured Output Generation.** SGLang (Zheng et al., 2024) optimizes structured output generation through techniques such as jump-forward decoding for deterministic tokens. Grammar-constrained approaches include Outlines (Willard & Louf, 2023) and XGrammar (Dong et al., 2024). While these methods improve output validity and efficiency, they remain fundamentally sequential. SimpleTool takes an orthogonal approach by reducing the output representation itself while enabling parallel generation across independent streams.

**Efficient LLM Serving.** Modern serving systems have improved LLM inference efficiency through various techniques. vLLM (Kwon et al., 2023) introduced PagedAttention for KV cache management, while SGLang (Zheng et al., 2024) proposed RadixAttention for prefix sharing. Quantization techniques such as AWQ (Lin et al., 2025) and GPTQ (Frantar et al., 2023) enable deployment on resource-constrained devices. SimpleTool is compatible with these optimizations and can be combined with existing serving infrastructure.

**Real-Time LLM Applications.** Vision-language-action models such as ST-2 (Zitkovich et al., 2023), OpenVLA (Kim et al., 2025), and  $\pi_0$  (Black et al., 2024) have demonstrated promising capabilities for robotic control. In game AI, Voyager (Wang et al., 2024a) and SIMA (SIMA Team et al., 2024) explore open-world control capabilities. For GUI automation, AutoDroid (Wen et al., 2024) and Mobile-Agent (Wang et al., 2024b) explore LLM-powered device control. These application domains commonly face latency challenges that motivate our work on parallel decoding.

## B. Special Token Definitions

SimpleTool introduces 17 special tokens organized into four functional groups. New tokens are appended to the vocabulary with IDs  $|\mathcal{V}_{\text{base}}|$  through  $|\mathcal{V}_{\text{base}}| + 16$ . Embeddings are initialized by averaging semantically similar existing tokens.

Table 7. Special token definitions and their functions.

Group	Tokens	Count
Content Control	<content>, </content>	2
Function Control	<function>, </function>	2
Argument Control	<arg $k$ >, </arg $k$ > for $k \in \{1, \dots, 6\}$	12
Placeholder	< null >	1
<b>Total</b>		<b>17</b>

**Example output format:**

```

<content>I'll check the weather for you.</content>
<function>get_weather</function>
<arg1>Beijing</arg1>
<arg2>2024-12-24</arg2>
<arg3>celsius</arg3>
<arg4><|null|></arg4>
<arg5><|null|></arg5>
<arg6><|null|></arg6>

```

## C. Parameter Count Statistics

We analyze the distribution of function parameter counts across all evaluation benchmarks to justify our design choice of 6 parallel argument heads.

### C.1. Distribution Analysis

Table 8 presents the number of samples with more than 6 parameters across all evaluation datasets (excluding SealTools 1–6 tools subsets, which are designed for controlled parameter count evaluation).

Table 8. Parameter count distribution across benchmarks. Samples with >6 parameters require sequential handling for additional arguments.

Dataset	Total	>6 params	Ratio	Max Params
BFCL-v3 Exec Multiple	50	0	0.00%	6
BFCL-v3 Exec Simple	100	0	0.00%	6
BFCL-v3 Live Multiple	1,053	167	15.86%	21
BFCL-v3 Live Simple	258	14	5.43%	10
BFCL-v3 Multiple	200	0	0.00%	6
BFCL-v3 Simple	400	0	0.00%	6
SealTools (in-domain)	199	4	2.01%	8
SealTools (out-domain)	94	0	0.00%	6
Mobile Actions	1,283	0	0.00%	4
OpenFunctions	109	0	0.00%	4
ToolAlpaca (real)	92	0	0.00%	6
ToolAlpaca (simulated)	51	0	0.00%	6
<b>Total</b>	<b>3,889</b>	<b>185</b>	<b>4.76%</b>	–

### C.2. Conclusion

Our default configuration of 6 parallel argument heads covers 95.2% of all function calls in the evaluated benchmarks. The 4.76% of cases with >6 parameters are concentrated in BFCL-v3 Live datasets, which contain real-world APIs with extensive optional parameters (e.g., REST APIs with many query parameters). For these cases, our model generates the first 6 arguments in parallel; additional arguments—typically optional—can be handled through sequential generation or omitted based on the tool schema’s `required` field specification.

Notably, all synthetic and controlled benchmarks (BFCL Non-Live, SealTools, Mobile Actions, OpenFunctions, ToolAlpaca) have a maximum of 6 parameters, confirming that our head count aligns with common API design practices.

## D. Training Data Statistics

**Argument distribution after augmentation:** 1 arg: 18%, 2 args: 20%, 3 args: 18%, 4 args: 17%, 5 args: 15%, 6 args: 12%. This balanced distribution addresses the natural imbalance where most real-world APIs use 1–2 arguments.

Table 9. Training data composition and statistics.

Source	Samples	Percentage
xLAM-60K (filtered)	48,000	40%
Synthetic (Qwen3-235B generated)	70,000	58%
Special (pass-through functions)	2,000	2%
<b>Total Groups</b>	<b>120,000</b>	<b>100%</b>
<b>Total Samples (<math>\times 8</math> heads)</b>	<b>960,000</b>	–

## E. Experimental Details

### E.1. Handling Parallel Tool Invocations

#### E.1.1. PROBLEM STATEMENT

Some benchmarks (e.g., Mobile Actions) contain samples with **parallel tool invocations**, where multiple functions are called simultaneously within a single turn. For example, a user request “Turn on my flashlight and show me the nearest bookstore on the map” expects two independent function calls:

```
tool_calls: [
  {"function": {"name": "turn_on_flashlight", "arguments": "{}"}},
  {"function": {"name": "show_map", "arguments": "{\"query\": \"nearest bookstore\""}}}
]
```

Since SimpleTool generates **one function call per inference pass**, we convert parallel invocations into sequential single-step evaluations using a history-based decomposition strategy.

#### E.1.2. CONVERSION STRATEGY

For  $K$  parallel tool calls  $\{c_1, c_2, \dots, c_K\}$ , we generate  $K$  training/evaluation samples. Each sample  $i$  receives:

- The original user query
- A `history` field containing preceding calls  $\{c_1, \dots, c_{i-1}\}$  (empty for the first entry)
- Ground truth expecting only call  $c_i$

**Key design choice for training:** During training data preparation, we apply **random shuffling** to the prefix calls for each version. This teaches the model that parallel calls have no inherent order dependency, which aligns with our parallel decoding assumption.

#### E.1.3. EXAMPLE

**Original** (2 parallel calls: `turn_on_flashlight`, `show_map`):

**Training Version 1** (target: `show_map`):

```
User: "Turn on flashlight and show nearest bookstore"
History: [turn_on_flashlight()]
Assistant: -> show_map(query="nearest bookstore") [TARGET]
```

**Training Version 2** (target: `turn_on_flashlight`):

```
User: "Turn on flashlight and show nearest bookstore"
History: [show_map(query="nearest bookstore")] [SHUFFLED]
Assistant: -> turn_on_flashlight() [TARGET]
```

#### E.1.4. IMPLEMENTATION

Algorithm 1 illustrates the conversion process.

**Algorithm 1** Parallel Tool Call Decomposition

---

**Require:** Sample with query  $q$ , tool definitions  $T$ , parallel calls  $C = \{c_1, \dots, c_K\}$

**Ensure:** Evaluation entries  $E = \{e_1, \dots, e_K\}$

```

1:  $E \leftarrow \emptyset$ 
2: for  $i = 1$  to  $K$  do
3:    $prefix \leftarrow \{c_1, \dots, c_{i-1}\}$ 
4:    $prefix \leftarrow \text{Shuffle}(prefix)$  {Random order for training}
5:    $history \leftarrow \text{Format}(prefix)$ 
6:    $query_i \leftarrow \text{Concat}(environment, history, q)$ 
7:    $gt_i \leftarrow \text{CreateGroundTruth}(c_i, T)$ 
8:    $e_i \leftarrow (query_i, T, gt_i)$ 
9:    $E \leftarrow E \cup \{e_i\}$ 
10: end for
11: return  $E$ 

```

---

### E.1.5. BENEFITS

1. **Data augmentation:**  $K$  parallel calls  $\rightarrow K$  training samples
2. **Order invariance:** Random shuffling teaches the model that parallel calls have no causal dependencies
3. **Complete coverage:** Every function in the parallel set is learned as a prediction target
4. **Consistent evaluation:** Each decomposed entry is evaluated independently; a parallel invocation is considered fully correct only if all  $K$  individual entries are correctly predicted

### E.2. Parameter Normalization

To ensure consistent evaluation across all benchmarks, we normalize tool definitions to have at most 6 parameters per function. Parameters are ordered as follows:

1. Required parameters in their original specification order
2. Optional parameters in alphabetical order

This normalization aligns with SimpleTool’s 6-argument head design and ensures that ground truth parameter ordering matches the tool definitions provided to the model.

### E.3. Latency Measurement Methodology

We measure inference latency using consistent methodology across all models and frameworks to ensure fair comparison.

#### Measurement Protocol.

- **Metric:** End-to-end wall-clock time from request submission to completion, including all framework overhead.
- **Warmup:** 5 requests discarded before measurement to ensure stable GPU state and cache initialization.
- **Sample size:** Full test split (1,283 samples for Mobile Actions) to capture latency distribution.
- **Statistics:** P50 (median) and P90 reported; P50 reflects typical performance while P90 captures tail latency.

**Framework Configuration.** All vLLM experiments use:

- `enable_prefix_caching=True`
- `gpu_memory_utilization=0.85`
- `tensor_parallel_size=1`
- Single request per batch (serial mode) to measure per-request latency rather than throughput

**Stop Token Configuration.** For SimpleTool models, we configure both string-based and token-ID-based stopping to ensure immediate termination on special tokens:

```
stop = ["<|null|>", "</function>", "</arg1>", ..., "<|im_end|>"]
stop_token_ids = [tokenizer.encode(s)[-1] for s in stop]
```

This dual configuration is critical for achieving optimal latency, as token-ID-based stopping triggers immediately upon generation without the 1-step delay inherent in string matching.

#### E.4. Mobile Actions Latency Benchmark Details

Table 10 provides comprehensive latency statistics for the Mobile Actions benchmark discussed in Section 3.4.

Table 10. Full latency statistics on Mobile Actions (1,283 samples, RTX 4090).

Model	P50 (ms)	P90 (ms)	P95 (ms)	P99 (ms)	Mean (ms)	Avg Tok
Qwen3-4B (Baseline)	468.5	667.0	731.2	845.3	489.7	39.2
Qwen2.5-0.5B (Baseline)	110.1	154.0	166.2	188.6	97.7	40.2
FunctionGemma (270M)	61.1	139.5	149.4	173.7	71.7	30.3
<b>ST-Qwen-0.5B (Ours)</b>	<b>51.0</b>	<b>74.5</b>	<b>82.2</b>	<b>90.0</b>	<b>50.1</b>	<b>~8</b>

#### Key Observations.

- ST-Qwen-0.5B achieves the lowest latency across all percentiles.
- The P90/P50 ratio for ST-Qwen-0.5B (1.27) is significantly lower than FunctionGemma (2.27), indicating more consistent performance.
- Average output tokens for ST-Qwen-0.5B (~8) are 3–5× fewer than baselines (30–40), directly contributing to reduced decode time.

#### E.5. Hardware Specifications

All experiments were conducted on the following hardware:

Table 11. Hardware configurations used in experiments.

Component	Specification
GPU	NVIDIA RTX 4090 (24GB VRAM)
GPU	NVIDIA H100/H200 (80GB/141GB VRAM)
CUDA	12.9
PyTorch	2.8.0
vLLM	0.12.0

Training experiments were conducted on H100/H200 GPUs. ST-Qwen-0.5B converges in approximately 3–4 H100-hours for initial training, and ~1 GPU-hour for domain adaptation on Mobile Actions.

## F. Training Hyperparameters

Table 12 presents the complete training configuration used for SimpleTool models. We highlight several key design choices:

**LoRA Configuration.** We target MLP layers (gate\_proj, up\_proj, down\_proj) rather than attention layers, as we find this provides greater capacity for learning the distinct output modes required by parallel heads. The relatively high rank ( $r = 512$ ) is necessary to capture diverse head-specific patterns without interference (see ablation in Section 3.5).

**Head Loss Weighting.** We apply higher weights to the function head ( $w_1 = 2.0$ ) since correct function selection is critical—an incorrect function name invalidates the entire output regardless of argument quality. Argument heads receive progressively increasing weights ( $w_2$  through  $w_7$ ) to counteract the natural data imbalance where higher-indexed arguments appear less frequently.

**Focal Weights.** For argument heads, we apply token-level focal weights that increase with head index. This addresses the challenge that later argument slots (arg4–arg6) have fewer training examples due to the skewed distribution of argument counts in real-world APIs.

Table 12. Complete training hyperparameters for SimpleTool in ST-Qwen3-4B

Parameter	Value
<i>LoRA Configuration</i>	
Rank ( $r$ )	512
Alpha ( $\alpha$ )	1024
Dropout	0.05
Target Modules	gate_proj, up_proj, down_proj
<i>Learning Rates</i>	
Embedding	$1 \times 10^{-6}$
LoRA	$1 \times 10^{-5}$
LM Head	$1 \times 10^{-6}$
Scheduler	Cosine with warmup
Warmup Ratio	0.02
<i>Training</i>	
Sequence Length	2048 tokens
Batch Size (per device)	8 groups
Gradient Accumulation	4 steps
Effective Batch Size	32 groups (256 samples)
Epochs	3–4
Precision	bfloat16
Flash Attention	Enabled (v2)
<i>Head Loss Weights (<math>w_h</math>)</i>	
$w_0$ (content)	0.01
$w_1$ (function)	2.0
$w_{2..7}$ (arg1–arg6)	1.1, 1.2, 1.3, 1.4, 1.5, 1.6
<i>Token-Level Focal Weights (<math>\gamma</math>, non-null only)</i>	
$\gamma_{2,3}$ (arg1–arg2)	1.0
$\gamma_4$ (arg3)	1.5
$\gamma_5$ (arg4)	2.0
$\gamma_6$ (arg5)	2.5
$\gamma_7$ (arg6)	3.0

## G. Batch Scaling Analysis

This appendix validates SimpleTool’s core assumption that parallel decoding incurs negligible overhead due to the memory-bandwidth-bound nature of autoregressive decoding.

### G.1. Experimental Setup

We measure per-token decode latency across varying batch sizes (1, 2, 4, 8, 16, 32, 64, 128) for six model configurations: Qwen2.5-0.5B, 1.5B, 3B, 7B, 14B, and Qwen3-4B. All experiments use identical input prompts and measure wall-clock time for the decode phase only, excluding prefill. We define **efficiency** as:

$$\text{Efficiency}(B) = \frac{T_d^{(B=1)}}{T_d^{(B)}} \quad (3)$$

where  $T_d^{(B)}$  is the per-token decode latency at batch size  $B$ . An efficiency of 100% indicates perfect scaling (no overhead from batching); lower values indicate compute saturation.

## G.2. Results

Table 13 presents efficiency across batch sizes. The key finding is that **8-head parallel decoding (corresponding to B=8) achieves 93.0% average efficiency**, with per-token overhead of only +8.2% compared to single-sequence decoding.

Table 13. Batch scaling efficiency (%) across model sizes. Higher values indicate better utilization of idle compute capacity. SimpleTool uses 8 heads, corresponding to B=8.

Model	B=1	B=2	B=4	B=8	B=16	B=32	B=64	B=128
Qwen2.5-0.5B	100.0	96.4	95.6	90.6	81.4	67.3	52.8	37.1
Qwen2.5-1.5B	100.0	98.3	97.5	92.7	86.5	78.7	64.7	47.1
Qwen2.5-3B	100.0	99.1	98.4	93.5	89.8	83.5	72.1	56.2
Qwen3-4B	100.0	98.7	96.3	92.5	83.7	74.4	58.1	45.8
Qwen2.5-7B	100.0	87.2	91.5	91.5	90.9	84.4	75.0	62.0
Qwen2.5-14B	100.0	99.3	98.4	97.4	95.2	90.6	78.1	66.5
<b>Average</b>	100.0	96.5	96.3	<b>93.0</b>	87.9	79.8	66.8	52.5

Table 14 presents the same data as wall-clock overhead relative to B=1.

Table 14. Wall-clock overhead (%) relative to single-sequence decoding (B=1). Lower values indicate less overhead from parallel execution.

Model	B=1	B=2	B=4	B=8	B=16	B=32	B=64	B=128
Qwen2.5-0.5B	+0.0	+3.7	+4.6	+10.3	+19.6	+34.5	+62.7	+125.3
Qwen2.5-1.5B	+0.0	+1.7	+2.6	+7.6	+15.6	+23.9	+44.4	+93.2
Qwen2.5-3B	+0.0	+0.9	+1.6	+6.9	+10.0	+19.1	+37.0	+76.9
Qwen3-4B	+0.0	+1.3	+3.9	+5.5	+10.4	+23.2	+37.6	+68.0
Qwen2.5-7B	+0.0	+12.8	+15.7	+16.3	+21.6	+26.6	+41.1	+68.7
Qwen2.5-14B	+0.0	+0.8	+1.7	+2.7	+4.7	+10.1	+23.2	+44.9
<b>Average</b>	+0.0	+3.5	+5.0	<b>+8.2</b>	+13.7	+22.9	+41.0	+79.5

## G.3. Analysis

**Memory-Bound Regime.** The high efficiency at B=8 confirms that autoregressive decoding operates in a memory-bandwidth-bound regime for typical model sizes. The GPU’s compute units remain underutilized during single-sequence decoding, allowing additional sequences to be processed with minimal latency increase.

**Efficiency Inflection Point.** Efficiency drops below 80% at  $B \geq 32$  for most models, indicating the transition from memory-bound to compute-bound regime. SimpleTool’s 8 parallel heads remain well within the “comfort zone” where parallelization overhead is negligible.

**Model Size Effect.** Larger models (7B, 14B) maintain higher efficiency at larger batch sizes, as their higher memory bandwidth requirements keep the system memory-bound for longer. This suggests SimpleTool’s parallel decoding strategy scales favorably with model size.

**Implications for SimpleTool.** With 8 parallel heads and +8.2% average overhead, the scheduling term  $T_o(H)$  in Equation 2 is effectively absorbed into a small multiplicative factor on  $T_d$ :

$$T_{\text{ours}} \approx T_p + \max_i(N_i) \cdot (1.08 \cdot T_d) \quad (4)$$

Combined with the 4–6 $\times$  token compression (Table 1), this yields the 3–6 $\times$  end-to-end speedup observed in Section 3.3.

## H. Token Compression Details

This appendix provides detailed token compression statistics supporting the analysis in Section 2.1.

Table 15. Detailed token compression analysis. BL = Baseline tokens, ST = ST bottleneck-head tokens, CR = Compression Ratio. All statistics computed on samples where both Baseline and ST models produce correct outputs.

Model	Mean			P50 (Median)			P90			N
	BL	ST	CR	BL	ST	CR	BL	ST	CR	
Qwen2.5-0.5B	44.1	8.7	5.06×	36.0	6.0	6.00×	69.0	17.0	4.06×	3328
Qwen2.5-1.5B	38.3	8.9	4.32×	33.0	7.0	4.71×	64.0	20.0	3.20×	3590
Qwen2.5-3B	39.2	8.9	4.38×	33.0	7.0	4.71×	64.0	20.0	3.20×	3939
Qwen3-4B <sup>†</sup>	38.4	8.9	4.32×	34.0	7.0	4.86×	65.0	19.0	3.42×	4074
Qwen2.5-7B	48.3	9.0	5.35×	35.0	7.0	5.00×	68.0	20.0	3.40×	4094
Qwen2.5-14B	40.2	8.9	4.51×	34.0	7.0	4.86×	66.0	19.0	3.47×	3946

<sup>†</sup>: Qwen3 backbone. N = number of both-correct samples.

## H.1. Methodology

We measure token compression by comparing output lengths between baseline models (generating full JSON-formatted function calls) and SimpleTool models (generating only value tokens across parallel heads). For SimpleTool, we report the **bottleneck head** token count—the maximum across all parallel heads—as this determines end-to-end latency per Equation 2.

Statistics are computed exclusively on samples where **both** baseline and SimpleTool models produce correct outputs, ensuring fair comparison on equivalent task difficulty. The compression ratio (CR) is defined as:

$$\text{CR} = \frac{\text{Baseline tokens}}{\text{ST bottleneck-head tokens}} \quad (5)$$

## H.2. Overall Results

Table 15 presents detailed statistics across model sizes, including mean, median (P50), and 90th percentile (P90) for both baseline and SimpleTool token counts.

Key observations:

- **Consistent compression across scales:** All models achieve 4.3–5.4× mean compression, indicating that the structural redundancy in function call outputs is model-agnostic.
- **Higher median than mean:** P50 compression (4.7–6.0×) exceeds mean compression, suggesting that outliers with longer outputs (complex nested arguments) pull down the average.
- **Stable RT token counts:** SimpleTool bottleneck-head tokens remain remarkably stable (8.7–9.0 mean) across model sizes, reflecting the consistent information content of function calls regardless of baseline verbosity.

## H.3. Per-Benchmark Breakdown

Table 16 presents compression ratios by benchmark group, revealing how compression varies across task types.

Key observations:

- **Highest compression on simple APIs:** BFCL Non-Live and OpenFunc achieve 5.7–7.9× compression, as these benchmarks feature functions with fewer, simpler arguments.
- **Lower compression on execution tasks:** BFCL Exec and MobileAct show 3.2–4.5× compression, reflecting more complex argument structures (e.g., nested objects, longer string values).
- **Outlier in ToolAlpaca:** Qwen2.5-7B achieves 20.54× compression on ToolAlpaca, likely due to baseline verbosity on specific samples; this outlier does not significantly affect overall conclusions.

## H.4. Relationship to End-to-End Speedup

The token compression ratio provides a **theoretical upper bound** on decode-phase speedup. The actual end-to-end speedup (3–6×, Section 3.3) is lower due to:

Table 16. Token compression ratio by benchmark group. CR = Compression Ratio (Baseline / RT). Results on both-correct samples. BFCL-NL = BFCL Non-Live, BFCL-L = BFCL Live, BFCL-E = BFCL Exec.

Model	BFCL-NL	BFCL-L	BFCL-E	SealTools	MobileAct	OpenFunc	ToolAlpaca	Overall
Qwen2.5-0.5B	7.05×	5.52×	4.53×	5.16×	4.17×	7.91×	5.14×	5.06×
Qwen2.5-1.5B	5.67×	5.00×	3.85×	4.51×	3.38×	5.19×	6.04×	4.32×
Qwen2.5-3B	5.73×	4.83×	3.55×	4.53×	3.73×	5.20×	4.48×	4.38×
Qwen3-4B <sup>†</sup>	5.71×	4.89×	3.16×	4.55×	3.54×	5.17×	4.47×	4.32×
Qwen2.5-7B	6.77×	6.43×	3.91×	5.97×	3.46×	5.29×	20.54×	5.35×
Qwen2.5-14B	5.81×	5.44×	3.38×	4.91×	3.31×	5.17×	6.16×	4.51×

<sup>†</sup>: Qwen3 backbone.

1. **Prefill overhead:**  $T_p$  is identical for both methods and does not benefit from token compression.
2. **Parallelization overhead:** The +8.2% overhead from 8-head parallel decoding (Appendix G).
3. **Framework overhead:** Scheduling, memory allocation, and other system-level costs in inference frameworks.

Despite these factors, SimpleTool achieves 70–80% of the theoretical compression-based speedup in practice, demonstrating efficient translation of token reduction into latency improvement.

## I. Limitations: Parameter Independence Assumption

### I.1. The Independence Assumption

Our parallel decoding assumes that function arguments are **conditionally independent** given the user query and function name:

$$P(\arg_1, \dots, \arg_k | q, f) \approx \prod_{i=1}^k P(\arg_i | q, f) \quad (6)$$

This assumption is justified by the design philosophy of JSON-based function calling: parameters are defined as unordered key-value pairs, and well-designed APIs treat each parameter as capturing an independent aspect of the request.

### I.2. Empirical Validation

Our benchmark results provide strong empirical support for this assumption:

- **Accuracy improvement:** SimpleTool achieves equal or higher accuracy than sequential baselines across all benchmarks (Table 2). If parameter dependencies were prevalent and important, removing sequential conditioning should *decrease* accuracy—the opposite of what we observe.
- **Order invariance in training:** Our parallel-to-multi-turn conversion (Appendix E.1) shuffles parameter order during training. The model’s strong performance indicates it learns to predict parameters independently of their presentation order.

### I.3. Theoretical Edge Cases

We acknowledge that some API designs could introduce parameter dependencies:

#### Example 1: Runtime-dependent validation

```
read_file_range(file_path, start_line, end_line)
```

Here, `end_line`’s validity depends on the actual file length. However, this is a *runtime* constraint, not a *generation* dependency—a sequential model would also generate `end_line=100` if the user requests it, regardless of whether the file has 100 lines.

#### Example 2: Cascading inference

```
format_convert(input_string, detected_format, output_format)
```

If `detected_format` must be inferred from `input_string`, this creates a true dependency. However:

1. This is poor API design—`detected_format` should be computed internally by the function, not passed as a parameter.
2. In practice, both values can often be inferred independently from context (e.g., “convert 2024-01-15 to MM/DD/YYYY” allows inferring both the input format and the input value).

#### I.4. Handling True Dependencies

For the rare cases where genuine parameter dependencies exist, SimpleTool supports two fallback strategies:

1. **Consolidation:** Dependent parameters can be combined into a single head as a structured value (e.g., a list or nested object).
2. **Multi-turn refinement:** For complex cases, the model can generate a partial call first, then refine in subsequent turns based on execution feedback.

#### I.5. Conclusion

The parameter independence assumption is both theoretically grounded (JSON’s key-value design) and empirically validated (accuracy improvements). While edge cases exist, they represent either poor API design or runtime constraints that affect sequential models equally. Our 95.2% benchmark coverage with 6 heads (Appendix C) further confirms that real-world APIs align with this assumption.

## J. Compatibility with Speculative Decoding

As discussed in Section 1, speculative decoding methods are orthogonal to SimpleTool: they accelerate per-token generation through draft-and-verify mechanisms, while we reduce the total number of tokens to generate. This appendix validates that these approaches can be combined for additional benefits.

### J.1. Experimental Setup

We evaluate speculative decoding on SimpleTool-trained models using the standard draft-model approach (Leviathan et al., 2023). The target model is ST-Qwen2.5-14B, with ST-Qwen2.5-0.5B and ST-Qwen2.5-1.5B serving as draft models. All models share the same special token vocabulary and output format, enabling direct speculation without format conversion.

We test speculation depths  $N \in \{2, 3, 4\}$  (number of tokens drafted per step) across all BFCL-v3 subsets and report forward pass reduction (vanilla forwards / speculative forwards) and token acceptance rate (accepted tokens / drafted tokens).

### J.2. Results

Table 17 summarizes the results across draft model sizes and speculation depths.

Table 17. Speculative decoding results with ST-Qwen2.5-14B as target. Speedup = forward pass reduction (higher is better). Accept Rate = proportion of drafted tokens accepted by target model.

Draft Model	N	Avg Speedup	Avg Accept Rate
ST-Qwen-0.5B	2	2.35×	95.0%
	3	2.83×	94.0%
	4	3.22×	93.6%
ST-Qwen-1.5B	2	2.37×	96.1%
	3	2.87×	95.5%
	4	3.24×	95.1%

Table 18 provides per-dataset breakdown for the best-performing configuration (ST-Qwen-1.5B draft,  $N = 4$ ).

Table 18. Per-dataset speculative decoding results (ST-Qwen-1.5B draft,  $N = 4$ ).

Dataset	Samples	Vanilla Fwds	Spec Fwds	Speedup	Accept Rate
BFCL-v3 Simple	400	6,578	2,031	3.24×	95.3%
BFCL-v3 Live Simple	244	4,698	1,401	3.35×	93.0%
BFCL-v3 Multiple	200	3,333	1,096	3.04×	96.1%
BFCL-v3 Live Multiple	886	17,196	6,593	2.61×	90.0%
BFCL-v3 Exec Simple	100	1,844	489	3.77×	98.2%
BFCL-v3 Exec Multiple	50	986	285	3.46×	98.1%
<b>Total/Average</b>	1,880	34,635	11,895	<b>3.24×</b>	<b>95.1%</b>

### J.3. Analysis

**High acceptance rates.** Both draft models achieve  $>93\%$  token acceptance rates across all configurations, significantly higher than typical speculative decoding scenarios on general text generation (70–85%). This is because SimpleTool’s simplified output format—consisting primarily of function names and argument values—exhibits lower entropy and higher predictability than free-form text, making smaller models more effective as drafters.

**Consistent speedup across datasets.** Forward pass reduction ranges from  $2.6\times$  to  $3.8\times$  depending on dataset complexity. Simpler datasets (Exec Simple/Multiple) achieve higher speedup due to more predictable outputs, while Live Multiple shows lower speedup due to greater output diversity.

**Draft model size trade-off.** The 1.5B draft model achieves slightly higher acceptance rates ( $+1\text{--}2\%$ ) than the 0.5B model, translating to marginally better speedup. However, the 0.5B model may be preferable for memory-constrained deployments where loading a larger draft model is impractical.

**Speculation depth trade-off.** Increasing  $N$  from 2 to 4 improves speedup from  $\sim 2.4\times$  to  $\sim 3.2\times$ , with only minor degradation in acceptance rate ( $\sim 1\%$ ). This suggests  $N = 4$  as a practical default for SimpleTool models.

### J.4. Combined Speedup Potential

The total theoretical speedup when combining SimpleTool with speculative decoding is multiplicative:

$$\text{Speedup}_{\text{combined}} = \text{CR} \times \text{Speedup}_{\text{spec}} \quad (7)$$

where CR is the token compression ratio from SimpleTool ( $4\text{--}6\times$ , Table 1) and  $\text{Speedup}_{\text{spec}}$  is the forward pass reduction from speculative decoding ( $2\text{--}3\times$ ).

For ST-Qwen2.5-14B with  $\text{CR} \approx 4.5\times$  (Table 1) and 1.5B draft model at  $N = 4$  ( $3.24\times$  forward reduction), the combined theoretical speedup reaches approximately **14.6×** in forward passes compared to vanilla autoregressive decoding of the baseline 14B model.

**Practical considerations.** While forward pass reduction provides a useful proxy for latency improvement, actual wall-clock speedup depends on additional factors: draft model inference overhead, verification batch size, and memory bandwidth utilization. For memory-bound inference on consumer GPUs, SimpleTool’s token compression alone often saturates available bandwidth, making speculative decoding most beneficial for larger models or datacenter deployments where compute becomes the bottleneck. We leave detailed wall-clock benchmarking of combined approaches to future work.

### J.5. Conclusion

These results confirm that SimpleTool and speculative decoding are complementary acceleration strategies operating on different axes: SimpleTool reduces *what* to generate (fewer tokens through compression and parallelization), while speculative decoding accelerates *how* to generate (fewer sequential forward passes through draft-and-verify). The exceptionally high acceptance rates ( $>93\%$ ) suggest that SimpleTool’s simplified output format is particularly amenable to speculative approaches, opening promising directions for further optimization.